RECIPROCAL SPACE IMAGING OF RADIATION-INDUCED DEFECTS IN BCC Fe

R.E. Stoller, G.E. Ice, R.I. Barabash

Metals and Ceramics Division, Oak Ridge National Laboratory, Oak Ridge TN 37831-6118

Abstract

It is important to determine the number and configuration of point defects that survive atomic displacement cascades in irradiated materials because only those defects that escape recombination are able to contribute to radiation induced property changes such as void swelling, hardening, embrittlement, and irradiation creep. Simulations of displacement cascades using molecular dynamics are being used to provide a description of the most probable surviving defects. In the case of interstitial-type defects in iron, these are predicted to be <110> and <111> type dumbbells and <111> crowdions, along with small clusters of these same defects. Diffuse x-ray and neutron scattering provides a direct method for obtaining detailed information on the displacement fields both near to and far away from the defects in addition to information on the particular position of the defect. To analyze such radiation damage with diffuse scattering, reciprocal space diffraction from crystals with variously oriented dumbbells and small clusters of dumbbells has been modeled. Diffuse scattering measurements between and close to Bragg reflections are sensitive to the orientation of the dumbbells, and the size and type of the small clusters at sizes that are too small to analyze by electron microscopy. Displacement of the near neighbors induces diffuse scattering in regions between the Bragg peaks, whereas the long range part of the displacement field results in Huang scattering close to the Bragg reflections. Simulation of diffuse scattering by different interstitial defects around (h00), (hh0), (hhh), (3h,h, 0) reflections demonstrates that each defect type leads to distinct isointensity contours. These scattering signatures can be used to determine the type and configuration of the surviving interstitials.

Introduction

In recent years, molecular dynamics (MD) simulations of high energy displacement cascades have provided a detailed picture of primary damage formation in irradiated materials [1-7]. An unanticipated observation in these studies was extensive formation of small interstitial clusters and the very high mobility exhibited by these clusters. In the case of iron, two primary stable interstitial configurations are found, the <110> and <111> dumbbells [3,4]. The difference in the formation energy between these configurations is only about 0.1 eV. The <111> dumbbell migrates with a low activation energy of ~0.1 eV, whereas the <110> dumbbell is essentially immobile near room temperature. The <110> dumbbell migrates by first rotating into a <111> dumbell. The interstitial clusters in iron are primarily clusters of <111> dumbbells, and they migrate with a low activation energy similar to that of the single <111> dumbbell, ~0.1 eV.

These interstitial properties are dependent on the interatomic potential employed, but similar results have been obtained with several different potentials. However, the iron potentials currently in use are isotropic, neglecting any directional effects that could arise from the unfilled d-electron orbitals in iron. This could have a significant effect on the interstitial properties predicted, and on any other model that makes use of these defect parameters. For example, extensive in-cascade clustering and low cluster mobility would give rise to a high density of

these clusters which would act as sinks for other mobile defects. Conversely, if the clusters are as mobile as they appear in the MD simulations, the defect concentrations would be relatively low since they would easily migrate to fixed sinks such as dislocations and grain boundaries [8]. Similarly, the higher mobility of <111> dumbbells implies that only <110> dumbbells should be observed following irradiation. The ultimate purpose of this work is to experimentally investigate the nature of the interstitial defects that are formed under neutron irradiation in order to evaluate the predictions of the MD models. To that end, a low-temperature neutron irradiation experiment of high-purity, nearly single crystal iron has been carried out. The results of the simulations discussed here will be used to guide subsequent examination of the irradiated specimen.

During the last two decades, the brilliance of the best x-ray sources has been doubling about every nine months. Recent progress in x-ray optics and commissioning of ultra brilliant third-generation synchrotron x-ray sources now allows for intense x-ray beams with 0.1 to 100 μm diameter spot size. These intense small beams enable experiments that were previously only possible with large single crystals. Diffuse scattering measurements are an example of this type of experiment.

Previous analysis of irradiation-induced point defects, defect clusters, and dislocation loops has been described in a number of papers [9-16]. Defect studies in iron are conducted less frequently than in the other materials [14, 15]. Small angle scattering [14] and measurements of electrical resistivity [15] have been used for the analysis of radiation induced defects in iron. Small angle scattering [14] is sensitive to variations in scattering-length density but is not sensitive to local distortions; interstitials in iron cause strong lattice distortions in the surrounding matrix. This work is intended to compute the expected diffuse scattering from realistic interstitial defect configurations with distortions that are highly anisotropic.

Simulation of Diffuse X-ray Scattering and Reciprocal Space Imaging

Defect configurations for the scattering simulations were prepared by MD. Simulations of single <110> and <111> dumbbells and clusters of five dumbbells of each type were carried out in cells of 128,000 atoms. The defect configurations were equilibrated at 100K and then quenched. The cluster configurations are shown in Fig. 1. In Fig.1 the larger green spheres are atoms displaced from a normal lattice site and the corresponding vacant lattice sites are shown as smaller red spheres lying between the atoms. In this case the dumbbells (two atoms sharing a single lattice site) have relaxed into the extended crowdion configuration (n atoms sharing n-1 lattice sites). The <111> cluster is typical of those obtained from high energy cascade simulations [1-4]. Since the MD simulations used periodic boundary conditions, one cluster in 128,000 atoms corresponds to a defect density of 7.8 appm. A simple kinetic model based on reaction rate theory was used to predict the interstitial cluster populations for two cases, one in which the clusters were as mobile as the single interstitial (migration energy 0.25 eV), and the other in which the clusters are assume to be immobile [8]. For the case of mobile clusters, the total cluster density was 10^{-6} appm, while a cluster density of 120 appm is predicted for the case of immobile clusters.

X-ray or neutron diffuse scattering is a powerful tool for measuring the structure and density of single dumbbell interstitials and clusters of these defect. The information obtained can reveal

the details of defect formation, particularly when a single defect type dominates. This information is often difficult or impossible to obtain with other methods.

The volume variation $\Delta V=\Delta V_i$ caused by an interstitial is larger by an order of magnitude than the modulus of the respective volume variation caused by vacancies $\Delta V=\Delta V_v$. The volume variation due to a split interstitial or dumbbell $\Delta V=\Delta V_d$ is even larger. Therefore diffuse scattering in the vicinity of the reciprocal lattice points (proportional to ΔV^2) and between the points is mainly sensitive to the interstitial-type defects.

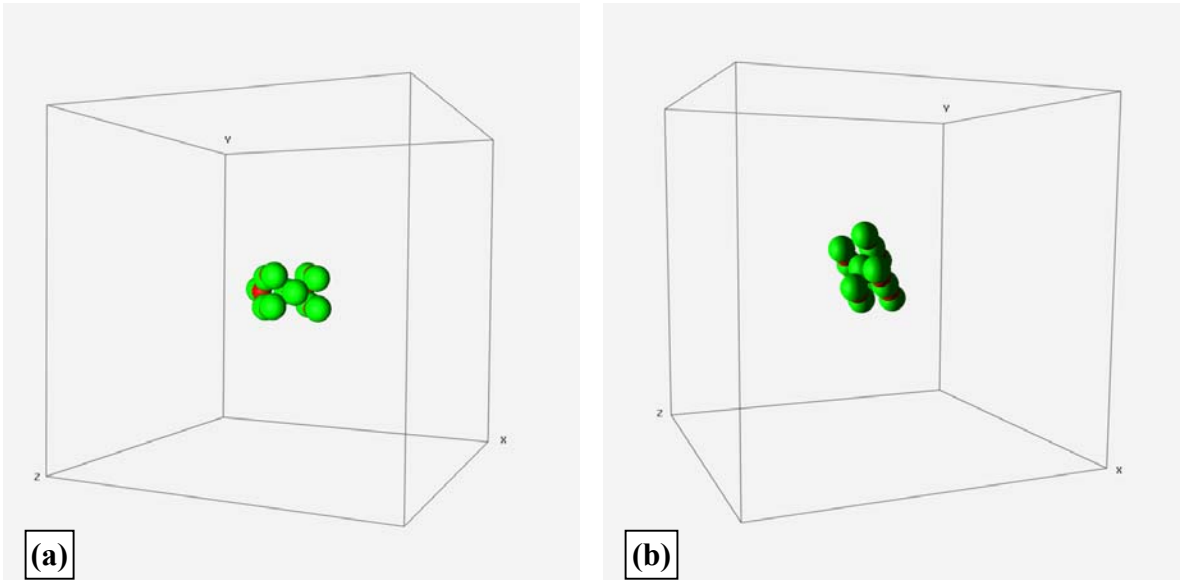

Fig. 1. Clusters of five <110> (a) and five <111> dumbbells (b) prepared by MD simulation.

For a small deviation ***q*** of the diffraction vector ***Q*** from reciprocal lattice point ***G:*** **q=Q-G**, the diffusely scattered intensity I_D is proportional to $1/q^2$. The asymmetric part of the scattering intensity varies as Q/q. The sign of the asymmetric term is determined by the sign of ΔV . For dumbbells that dilate the lattice, the diffuse scattering intensity is larger at larger scattering angles than for smaller angles. Simulated contour maps at different plane sections of the reciprocal space in the region containing 5x5 reciprocal unit cells are shown in Figs. 2 and 3 for <110> and <111> type dumbbells. The X, Y and Z axes correspond to [100], [010] and [001] directions of the reciprocal space. Note that the XY, XZ and YZ plane sections differ for [110] dumbbells and depend on the orientation of the dumbbell axis. In the case of [111] type dumbbells all the above three sections are identical (Fig. 3a, 4a).

When n_0 individual dumbbells aggregate into a cluster the "strength" coefficient C of the defect increases by approximately a factor of n_0. At small distances from the cluster the displacements may be quite considerable. Therefore, the proportionality $\boldsymbol{I_D \alpha 1/q^2}$ is applicable in a significantly smaller range than in the case of individual dumbbells and outside this range I_D decreases at a much faster rate and in some cases $\boldsymbol{I_D \alpha 1/q^4}$. Usually clusters contain the same type of dumbbells with their axes parallel to each other. Displacement fields around such a cluster are

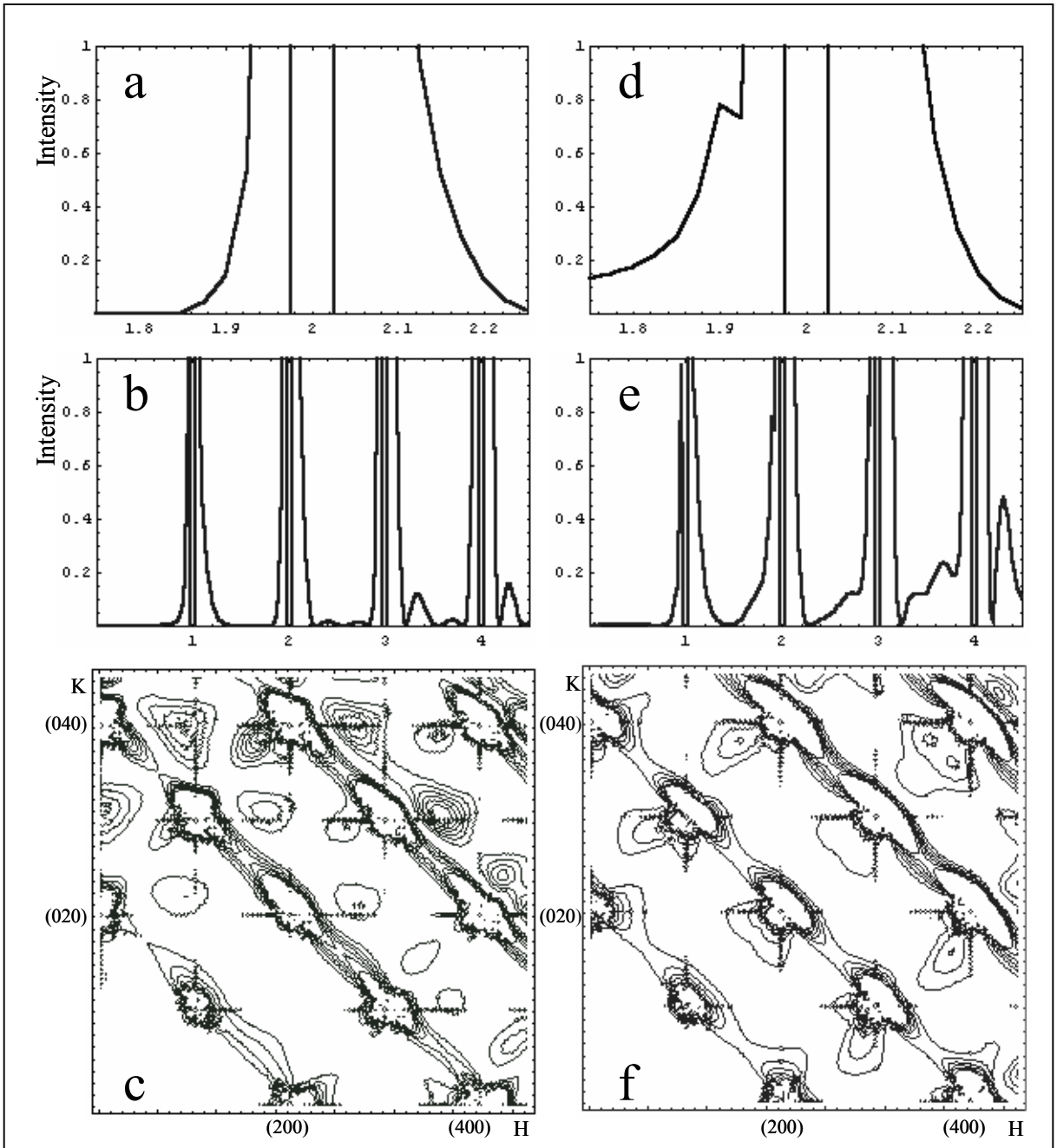

Fig.2. Intensity profiles along [H00] (a,b) and [HH0] (d,e) directions, and contourmaps (c,f) of scattered intensity at the planes XY(left) and YZ (right) due to [110] type dumbbells

highly anisotropic and result in much larger asymmetry of the scattered intensity. The equal intensity contours for a single [111] dumbbell and for a clusters containing 5 parallel [111] dumbbells are presented in Fig. 4. The increase in the number n_0 of dumbbells in the cluster causes additional asymmetry between XY, XZ and YZ plane sections of the reciprocal space.

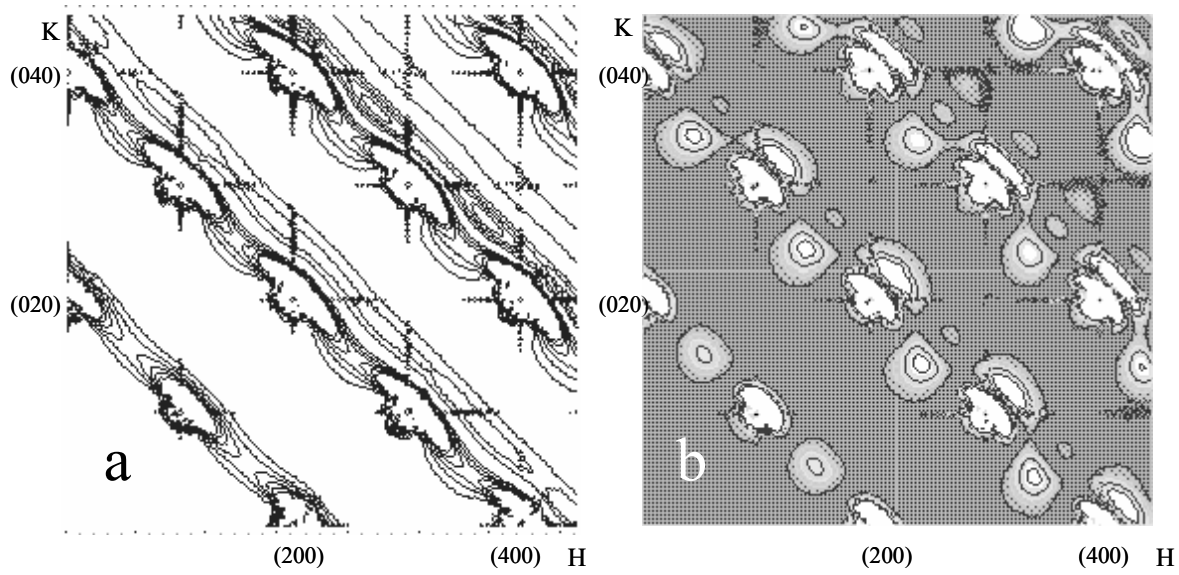

Fig. 3. Contour maps of equal intensity lines from a single [111] dumbbell (a), and a cluster from 5 parallel [111] dumbbells. Section at YZ plane at x=0

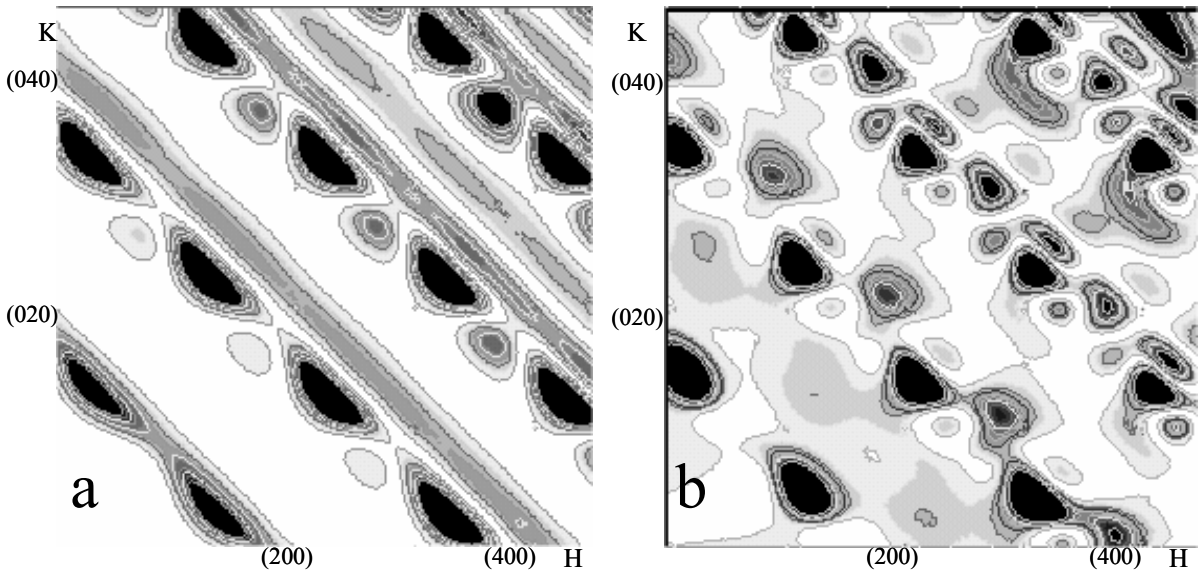

Fig. 4. Contour maps of equal intensity lines from a single [111] dumbbell (a), and a cluster from 5 parallel [111] dumbbells. Section at YZ plane at x=0.5

Summary

Modern synchrotron x-ray sources with high intensity and small spot sizes permit the measurement of diffuse scattering far from fundamental reflections and to separate the thermal and static displacement input into scattering. Based on interstitial defect configurations obtained

from molecular dynamics simulations, and the calculated defect density for the irradiated specimen mentioned above, we expect that:

1. Measurement of diffuse scattering will permit the determination of the symmetry of the dumbbell interstitial, i.e. <110> vs. <111>, in iron,

2. An upper limit on the interstitial defect density can be inferred from the scattering data which can help confirm or refute the high defect mobility observed in the MD simulations, and

3. The extent of interstitial clustering of the dumbbells can be determined due to an increase of both the magnitude and the asymmetry of diffuse scattering for clusters relative to the single defect.

This use of diffuse x-ray scattering can provide details on the primary damage state in irradiated materials when the defect sizes are too small to be seen by methods such as TEM. Thus, the use of the new x-ray sources should be encouraged as a tool for the analysis of irradiation effects.

Acknowledgements

Research sponsored by the Office of Fusion Energy Sciences and the Division of Materials Sciences and Engineering, U.S. Department of Energy under contract DE-AC05-00OR22725 with UT-Battelle, LLC.

References

1. R. E. Stoller and A. F. Calder, J. Nucl. Mater. **283-287**, 746-752 (2000).

2. W. J. Phythian, R. E. Stoller, A. J. E. Foreman, A. F. Calder, and D. J. Bacon, J. Nucl. Mater. **223,** 245 (1995).

3. R. E. Stoller, G. R. Odette, and B. D. Wirth, J. Nucl. Mater. **251**, 49-69 (1997).

4. R. E. Stoller, J. Nucl. Mater. **276**, 22-32 (2000).

5. D. J. Bacon, F. Gao, and Yu. N. Osetsky, J. Nucl. Mater. **276** (2000) 1-12.

6. M. J. Caturla, N. Soneda, E. Alonso, B. D. Wirth, T. Diaz de la Rubia, and J. M. Perlado, J. Nucl. Mater. **276**, 13-21 (2000).

7. K. Nordlund and R. S. Averback, J. Nucl. Mater. **276**, 194-201 (2000).

8. R. E. Stoller, "The Impact of Mobile Defect Clusters in a Kinetic Model of Pressure Vessel Embrittlement," Effects of Radiation on Materials, ASTM STP-1325, ASTM International, West Conshohocken, PA, pp. 15-29, 1999.

9. H.G. Haubold, Revue de Physique Appliquee **11**, 73-81 (1976).

10. B.C. Larson, J. Appl. Cryst. **8**,150-160 (1975).

11. B.C. Larson and F.W. Young, Jr., Phys. Stat. Sol. (a) **104,** 273-286 (1987).

12. B.C. Larson and W. Schmatz, Phys. Stat. Sol. (b) **99**,267-275 (1980).

13. B. Schonfeld and P. Ehrhart, Phys. Rev. B. **19**, 3905-3910 (1979).

14. H. Franz, G. Wallner and J. Peisl, Rad. Eff. and Def. in Solids **128**, 189-204 (1994).

15. H. Abe and E. Kuramoto, J. Nucl. Mater. **283-287**, 174-178 (2000).

16. H. Peisl, J. Appl. Cryst. **8**, 143-149 (1975).